arXiv:1411.4865v1 [hep-ex] 18 Nov 2014

SNSN-323-63
November 19, 2014

Measurement of CP observables in $B_s^0 \to D_s^{\mp} K^{\pm}$ at LHCb

Vladimir Gligorov
On behalf of the LHCb collaboration

CERN
Geneva, Switzerland

The time-dependent CP-violating observables accessible through $B_s^0 \to D_s^{\mp} K^{\pm}$ decays have been measured for the first time using data corresponding to an integrated luminosity of 1 fb^{-1} collected in 2011 by the LHCb detector. The CP-violating observables are found to be: $C_f = 0.53 \pm 0.25 \pm 0.04$, $A_f^{\Delta\Gamma} = 0.37 \pm 0.42 \pm 0.20$, $A_{\overline{f}}^{\Delta\Gamma} = 0.20 \pm 0.41 \pm 0.20$, $S_f = 1.09 \pm 0.33 \pm 0.08$, $S_{\overline{f}} = 0.36 \pm 0.34 \pm 0.08$, where the first uncertainty is statistical and the second systematic. Using these observables, the CKM angle γ is determined to be $(115^{+28}_{-43})^\circ$ modulo 180° at 68% CL, where the uncertainty contains both statistical and systematic components.

PRESENTED AT

The 8th International Workshop on the CKM Unitarity Triangle (CKM 2014)
Vienna, Austria, September 8-12, 2014

1 Introduction

Matter-antimatter asymmetry (CP violation) in weak interactions is described by a single, irreducible phase in the Cabibbo-Kobayashi-Maskawa (CKM) quark mixing matrix [1, 2]. As this is a 3×3 unitary, hermitian, matrix, it can be represented as a "Unitarity Triangle" in the complex plane. Since the matter-antimatter asymmetry in the Standard Model is too small [3] to account for the disappearance of antimatter following the Big Bang, it is reasonable to suppose that the Standard Model picture of CP violation is not self-consistent and breaks down at some level. By experimentally overconstraining the Unitarity Triangle, we are therefore directly probing the energy scale of potential physics beyond the Standard Model.

The time-dependent decay rates of the $|B_s^0(t=0)\rangle$ and $|\overline{B}_s^0(t=0)\rangle$ flavour eigenstates to final state f are:

$$\frac{d\Gamma_{B_s^0 \to f}(t)}{dt} \propto e^{-\Gamma_s t}[cosh(\tfrac{\Delta\Gamma_s t}{2}) + A_f^{\Delta\Gamma} sinh(\tfrac{\Delta\Gamma_s t}{2}) + C_f cos(\Delta m_s t) - S_f sin(\Delta m_s t)],$$
$$\frac{d\Gamma_{\overline{B}_s^0 \to f}(t)}{dt} \propto e^{-\Gamma_s t}[cosh(\tfrac{\Delta\Gamma_s t}{2}) + A_f^{\Delta\Gamma} sinh(\tfrac{\Delta\Gamma_s t}{2}) - C_f cos(\Delta m_s t) + S_f sin(\Delta m_s t)].$$

Similar decay rates hold for the conjugate processes. In the case where $f \equiv D_s^- K^+$, the four decay rates give five independently measureable CP-violating observables ("CP observables" henceforth), which are related to $r_{D_s K} \equiv |A(\overline{B_s}^0 \to D_s^- K^+)/A(B_s^0 \to D_s^- K^+)|$, the ratio of the magnitudes of the interfering diagrams, as well as the strong phase difference δ and the weak phase difference $\gamma - 2\beta_s$:

$$C_f = \tfrac{1-r_{D_s K}^2}{1+r_{D_s K}^2},\ A_f^{\Delta\Gamma} = \tfrac{-2r_{D_s K}\cos(\delta-(\gamma-2\beta_s))}{1+r_{D_s K}^2},\ A_{\overline{f}}^{\Delta\Gamma} = \tfrac{-2r_{D_s K}\cos(\delta+(\gamma-2\beta_s))}{1+r_{D_s K}^2},$$
$$S_f = \tfrac{2r_{D_s K}\sin(\delta-(\gamma-2\beta_s))}{1+r_{D_s K}^2},\ S_{\overline{f}} = \tfrac{-2r_{D_s K}\sin(\delta+(\gamma-2\beta_s))}{1+r_{D_s K}^2},$$

where $\beta_s \equiv \arg(-V_{ts}V_{tb}^*/V_{cs}V_{cb}^*)$. These observables can therefore be used to measure γ, an angle of the Unitarity Triangle, with negligible [4] theoretical uncertainty.

2 Cancellation of ambiguities

As discussed in [5], the fact that $\Delta\Gamma_s$ is relatively large makes both the sinusoidal and hyperbolic CP observables in $B_s^0 \to D_s^\mp K^\pm$ measurable and hence results in only a twofold ambiguity on the measured value of the CKM angle γ and the strong phase difference δ. In order to illustrate this point, it is useful to consider the constraints on γ due to each of the observables listed in Eq. 1. These are illustrated in Fig. 1, which clearly shows how the diagonal staggering of the sinusoidal and hyperbolic constraints in the $\delta - \gamma$ plane cancels all but one of the ambiguous solutions.

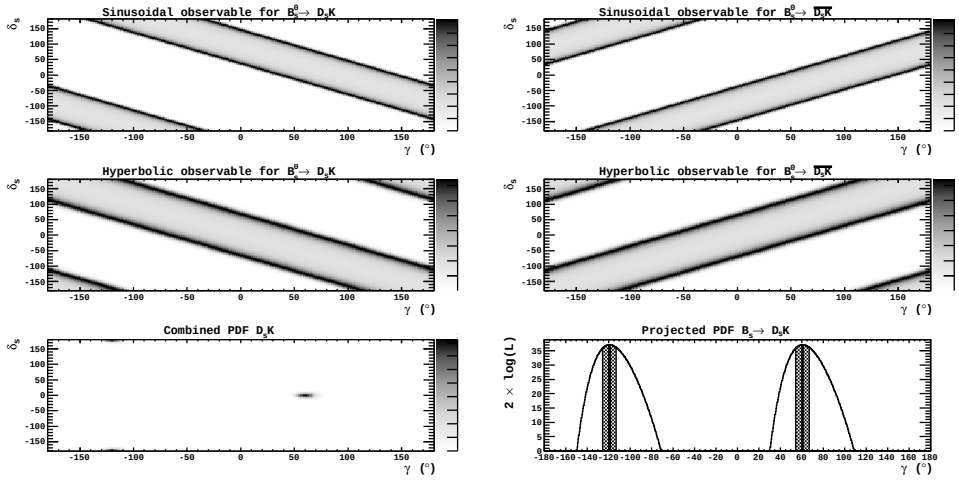
Sinusoidal observable for $B_s^0 \to D_s K$
Sinusoidal observable for $B_s^0 \to \overline{D_s} K$
Hyperbolic observable for $B_s^0 \to D_s K$
Hyperbolic observable for $B_s^0 \to \overline{D_s} K$
Combined PDF $D_s K$
Projected PDF $B_s \to D_s K$
δ_s
γ (°)
$2 \times \log(L)$

Figure 1: Reproduced from [6]. The top four plots show the likelihoods of the CP observables with 31k signal events and LHCb MC performance [7]. The bottom left plot shows the combined likelihood in the $\gamma - \delta_s$ plane and the bottom right the projection onto γ, where the hatched area is the 1σ region and the dark vertical line the central value. All but two of the ambiguities are excluded.

3 Event selection

The analysis uses a datasample corresponding to an integrated luminosity of 1 fb^{-1} collected by LHCb detector in 2011. The full description of detector can be found in [8]. The trigger [9] consists of a hardware stage, based on information from the calorimeter and muon systems, followed by a software stage, in which all charged particles with $p_T > 500$ MeV are reconstructed, and a multivariate algorithm [10] is used to select displaced vertices compatible with the decay of a b-hadron.

The D_s^- particle is reconstructed in three decay modes: $D_s^- \to K^-K^+\pi^-$, $D_s^- \to K^-\pi^+\pi^-$, and $D_s^- \to \pi^-\pi^+\pi^-$. These D_s^- candidates are subsequently combined with a fourth particle, referred to as the "companion", to form $B_s^0 \to D_s^\mp K^\pm$ and $B_s^0 \to D_s^-\pi^+$ candidates. The flavour-specific Cabibbo-favoured decay mode $B_s^0 \to D_s^-\pi^+$ is used as a control channel for the analysis, in particular for optimizing the selection and constraining the decay-time-dependent selection efficiency.

The different D_s^- final states are distinguished by a combination of particle identification information from LHCb's Ring Imaging Cherenkov (RICH) subdetectors and kinematic vetoes. This selection also strongly suppresses cross-feed and peaking backgrounds from other misidentified decays of b-hadrons to c-hadrons.

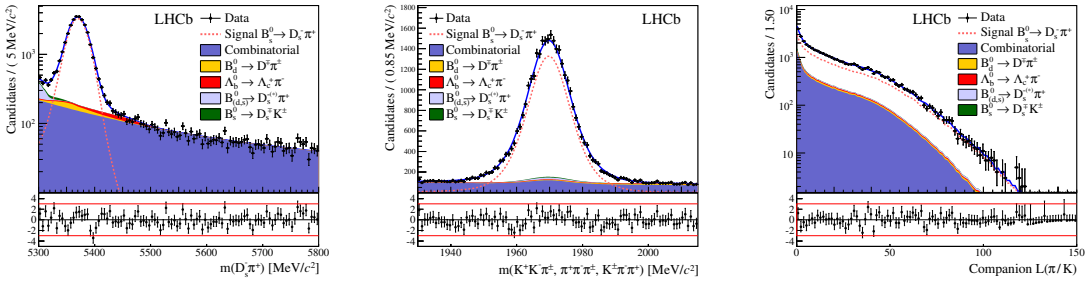

Figure 2: Multivariate fit to all $B_s^0 \to D_s^- \pi^+$ candidates.Left to right: distributions of candidates in B_s^0 mass, D_s^- mass, companion PID log-likelihood difference.

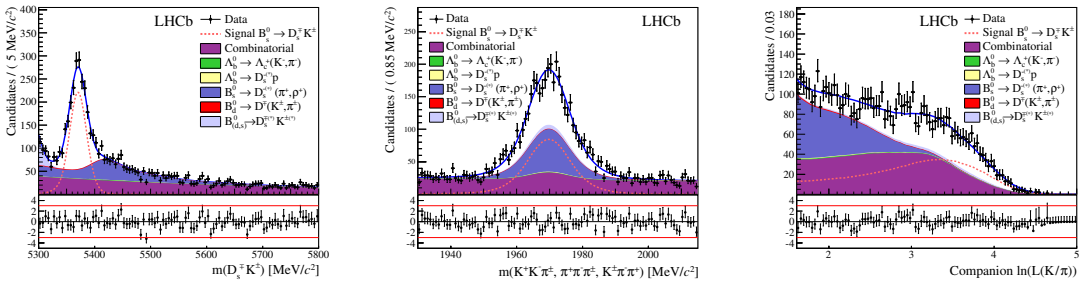

Figure 3: Multivariate fit to all $B_s^0 \to D_s^\mp K^\pm$ candidates.Left to right: distributions of candidates in B_s^0 mass, D_s^- mass, companion PID log-likelihood difference.

4 Multivariate fit to $B_s^0 \to D_s^\mp K^\pm$ and $B_s^0 \to D_s^- \pi^+$

The signal and background yields in the $B_s^0 \to D_s^\mp K^\pm$ and $B_s^0 \to D_s^- \pi^+$ channels are determined using a three-dimensional simultaneous extended maximum likelihood fit in the B_s^0 mass, the D_s^- mass, and the log-likelihood difference $L(K/\pi)$ between the pion and kaon hypotheses for the companion particle. Correlations between the fitting variables are shown to be negligible using simulated events.

The dominant backgrounds are random combinations of D_s^- mesons with pions or kaons, partially reconstructed decays of the type $B_s^0 \to D_s^-(\pi, K)^+ X$, and decays of B^0 and Λ_b hadrons in which the D^+ or Λ_c candidates are misidentified as D_s^- candidates. Most background yields float in the fit, with the exception of modes with yields below 2% of the signal yield which are fixed from known branching fractions and relative efficiencies measured using simulated events. The multivariate fit results in a signal yield of $28\,260 \pm 180$ $B_s^0 \to D_s^- \pi^+$ and 1770 ± 50 $B_s^0 \to D_s^\mp K^\pm$ decays, shown in Fig. 2 and Fig. 3, respectively. The multivariate fit is checked for biases using large samples of data-like pseudoexperiments, and none are found.

5 Inputs to the time-dependent fit

The measurement of the sinusoidal components of the $B_s^0 \to D_s^{\mp} K^{\pm}$ decay rates requires the determination ("tagging") of the initial flavour of the B_s^0 meson. The performance of the LHCb flavour tagging algorithms is described in detail in [11]. This analysis uses two types of taggers: opposite side, which infer the production flavour of the B_s^0 meson by partially reconstructing the other b-hadron produced in the pp collision; and same-side, which infer the production flavour of the B_s^0 meson by finding a charged kaon produced in the same fragmentation chain. The total tagging efficiency is 67.53% and the total effective tagging power is 5.07%.

The decay-time of the B_s^0 candidate is computed using a kinematic fit which constrains the mass of the D_s^- meson to the world-average value, as well as constraining the B_s^0 candidate to point to the associated pp collision vertex. This fit also returns an estimated per-event decay-time uncertainty, which is used as an observable when fitting to the decay rates in order to maximize sensitivity. The estimated decay-time uncertainty is calibrated using prompt D_s^- mesons which are combined with a random track and kinematically weighted to give a sample of "fake B_s^0" candidates, and the scale factor is found to be 1.37 ± 0.10.

Because the hyperbolic CP observables in $B_s^0 \to D_s^{\mp} K^{\pm}$ are fully correlated with the decay-time acceptance, it must be independently measured and fixed in the fit. This is done using the known value of Γ_s and the $B_s^0 \to D_s^- \pi^+$ control channel. The obtained acceptance is corrected by the acceptance ratio of $B_s^0 \to D_s^{\mp} K^{\pm}$ and $B_s^0 \to D_s^- \pi^+$ found in simulation. In order to help fit stability and speed, the decay-time acceptance is implemented using analytically integrable spline polynomials [12].

Finally, the following paremeters are fixed from independent measurements [13, 14, 15]: $\Gamma_s = (0.661 \pm 0.007) ps^{-1}$, $\Gamma_{\Lambda_b^0} = (0.676 \pm 0.006) ps^{-1}$, $\Delta\Gamma_s = (0.106 \pm 0.013) ps^{-1}$, $\Gamma_d = (0.658 \pm 0.003) ps^{-1}$, $\Delta m_s = (17.768 \pm 0.024) ps^{-1}$, $\rho(\Gamma_s, \Delta\Gamma_s) = -0.39$,
where $\rho(\Gamma_s, \Delta\Gamma_s)$ is the correlation between these two measurements, $\Gamma_{\Lambda_b^0}$ the Λ_b^0 decay-width, Γ_d the B_d^0 decay width, and Δm_s the B_s^0 oscillation frequency.

6 Time-dependent fit to $B_s^0 \to D_s^{\mp} K^{\pm}$

The determination of the CP observables is performed using two different unbinned maximum likelihood fits. In the first (*cFit*) all signal and background time distributions are described. In the second (*sFit*) the background is statistically subtracted using the *sPlot* technique [16] and only the signal time distributions are described. The signal decay-time model is identical in the two fitters.

Decay-time PDFs for both signal and background components account for flavour tagging, are convolved with a single Gaussian representing the per-candidate decay-time resolution, and are multiplied by the decay-time acceptance. In the *sFit* ap-

proach the signal $B_s^0 \to D_s^{\mp} K^{\pm}$ model is fitted to the three time-dependent observables: decay time, decay-time uncertainty, and predicted mistag. In order to optimally discriminate against background, the *cFit* performs a six-dimensional fit to the time-dependent observables and the three observables used in the multivariate fit.

The results of the *cFit* and *sFit* for the CP observables are given in Table 1, and shown in Fig. 4. Systematic uncertainties divide into three kinds: uncertainties from the fixed parameters, uncertainties from the limited knowledge of the decay-time resolution and acceptance, and uncertainties related to fit biases. The first two are estimated using large sets of simulated pseudoexperiments, in which the relevant parameters are varied within their uncertainty. The third is computed by splitting the data into independent subsamples, repeating the entire analysis chain for each one, and comparing the weighted average of the results to the nominal result. The measurement is statistically limited, and the largest systematic uncertainties are on the hyperbolic observables, due to the limited knowledge of Γ_s, $\Delta\Gamma_s$, and the decay-time acceptance.

Table 1: Fitted CP observables for (left) *sFit* and (right) *cFit*. The first uncertainty is statistical and the second is systematic.

Parameter	sFit fitted value	cFit fitted value
C_f	$0.52 \pm 0.25 \pm 0.04$	$0.53 \pm 0.25 \pm 0.04$
S_f	$-0.90 \pm 0.31 \pm 0.06$	$-1.09 \pm 0.33 \pm 0.08$
$S_{\overline{f}}$	$-0.36 \pm 0.34 \pm 0.06$	$-0.36 \pm 0.34 \pm 0.08$
$A_f^{\Delta\Gamma}$	$0.29 \pm 0.42 \pm 0.17$	$0.37 \pm 0.42 \pm 0.20$
$A_{\overline{f}}^{\Delta\Gamma}$	$0.14 \pm 0.41 \pm 0.18$	$0.20 \pm 0.41 \pm 0.20$

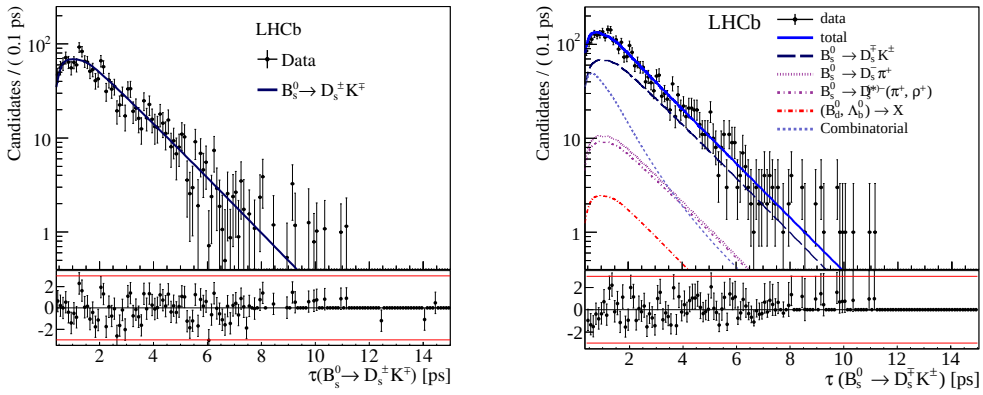

Figure 4: The (top) *sFit* and (bottom) *cFit* to the $B_s^0 \to D_s^{\mp} K^{\pm}$ candidate decay-time.

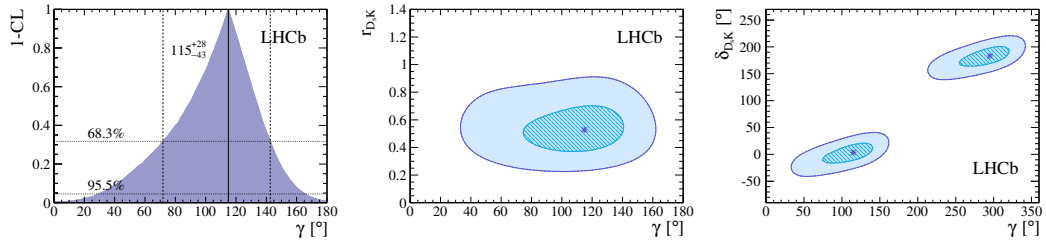

Figure 5: 1-CL for γ, together with the central value and the 68.3% CL interval (left). Profile likelihood contours of r_{D_sK} vs. γ (middle), and δ vs. γ (bottom). The contours are at 1σ (2σ), corresponding to 39% CL (86% CL) in the Gaussian approximation. The markers denote the best-fit values.

As the *cFit* and *sFit* sensitivities are very similar, the nominal result was randomly chosen to be the *cFit*.

7 Determination of the CKM γ angle

The measurement of the CP observables is interpreted in terms of $\gamma - 2\beta_s$ by maximising

$$\mathcal{L}(\vec{\alpha}) = exp(-\tfrac{1}{2}(\vec{A}(\vec{\alpha}) - \vec{A}_{obs})^T V^{-1}(\vec{A}(\vec{\alpha}) - \vec{A}_{obs})), \qquad (5)$$

where $\overrightarrow{\alpha} = (\gamma, \phi_s, r_{D_sK}, \delta)$ is the vector of the physics parameters, $\vec{A}$ is the vector of observables, $\vec{A}_{obs}$ is the vector of the measured CP observables and V is the experimental (statistical and systematic) covariance matrix.

The value of mixing phase is constrained by $-2\beta_s = \phi_s = 0.01 \pm 0.07(stat) \pm 0.01(syst)\ rad$ from the LHCb measurement of $B^0_s \to J/\phi K^+K^-$ and $B^0_s \to J/\phi\pi^+\pi^-$ decays [15]. This assumes that penguin pollution and BSM contributions are negligible, which is certainly a good approximation at the present statistical sensitivity.

Confidence intervals are computed using a frequentist method, and found to be:

$$\gamma = (115^{+28}_{-43})^\circ,$$
$$\delta_{D_sK} = (3^{+19}_{-20})^\circ,$$
$$r_{D_sK} = 0.53^{+0.17}_{-0.16},$$

where the intervals for the angles are expressed modulo 180°. Fig. 5 shows the $1-$CL curve for γ, and the two-dimensional contours of the profile likelihood.

8 Conclusion

The time-dependent CP observables accessible through $B^0_s \to D^\mp_s K^\pm$ decays have been measured for the first time and found to be: $C_f = 0.53 \pm 0.25 \pm 0.04$, $A^{\Delta\Gamma}_f = 0.37 \pm$

0.42 ± 0.20, $A_{\overline{f}}^{\Delta\Gamma} = 0.20 \pm 0.41 \pm 0.20$, $S_f = 1.09 \pm 0.33 \pm 0.08$, $S_{\overline{f}} = 0.36 \pm 0.34 \pm 0.08$, where the first uncertainty is statistical and the second systematic. Using these observables, the CKM angle γ is determined to be $(115^{+28}_{-43})^\circ$ modulo 180° at 68% CL, where the uncertainty contains both statistical and systematic components.

ACKNOWLEDGEMENTS

This analysis took several years and was a huge collaborative effort, and I would like to express my thanks and appreciation to the $B_s^0 \to D_s^\mp K^\pm$ analysis team: Suvayu Ali, Agnieszka Dziurda, Till Moritz Karbach, Rose Koopman, Eduardo Rodrigues, Manuel Schiller, Maximillian Schlupp, Giulia Tellarini, and Stefania Vecchi. I would also like to give a special thanks to the subdetector and computing teams of the LHCb collaboration, without whom none of our physics analyses would see the light of day.

References

[1] N. Cabibbo, Phys. Rev. Lett. 10 (1963) 531.

[2] M. Kobayashi and T. Maskawa, Prog. Theor. Phys. 49 (1973) 652.

[3] P. Huet and E. Sather, Phys. Rev. D **51** (1995) 379.

[4] J. Brod and J. Zupan, JHEP **1401** (2014) 051.

[5] R. Fleischer, Nucl. Phys. B671 (2003) 459.

[6] V. V. Gligorov, Proceedings of CKM 2010.

[7] K. Akiba *et al.*, CERN-LHCB-2008-031.

[8] LHCb collaboration, A. A. Alves Jr. et al., JINST **3** (2008) S08005.

[9] R. Aaij et al., JINST **8** (2013) P04022.

[10] V. V. Gligorov and M. Williams, JINST **8** (2013) P02013

[11] M.Dorigo, Proceedings of ICHEP 2014.

[12] T. M. Karbach, G. Raven and M. Schiller, arXiv:1407.0748.

[13] LHCb collaboration, R. Aaij et al., New J. Phys. 15 (2013) 053021,

[14] Particle Data Group, J. Beringer et al., Phys. Rev. D86 (2012) 010001.

[15] LHCb collaboration, R. Aaij et al., Phys. Rev. D87 (2013) 112010.

[16] M. Pivk and F. R. Le Diberder, Nucl. Instrum. Meth. A555 (2005) 356.